Nuclear Instruments and Methods in Physics Research B32 (1988) 32–36
North-Holland, Amsterdam

MICROSTRUCTURE OF Fe IMPLANTED YTTRIA STABILISED ZIRCONIA STUDIED BY MÖSSBAUER SPECTROSCOPY AND TEM

A.J. BURGGRAAF, D. SCHOLTEN and B.A. van HASSEL

University of Twente, Faculty of Chemical Engineering, Laboratory of Inorganic Chemistry, Materials Science and Catalysis, P.O. Box 217, 7500 AE Enschede, The Netherlands

Single crystalline and ceramic solid solutions of $(1-0.x)(ZrO_2)$–$(0.x)(YO_{1.5})$ with $x = 14$–17 were implanted with high doses of Fe. Specific profile shapes were realised. The microstructure of the material before and after annealing was studied by conversion electron Mössbauer spectroscopy (CEMS), ion channeling and transmission electron microscopy (TEM).

Initially Fe is present as metallic particles Fe^0 and as Fe^{2+} and Fe^{3+} ions. Their relative abundancy depends on the implantation conditions. Annealing leads to complete oxidation (Fe^{3+}) at low temperature and to the formation of microprecipitates of Fe_2O_3 (< 5 nm). A maximum of 4.5×10^{21} Fe cm^{-3} can be substitutionally incorporated for Zr. This Fe is present in a metastable state. Ion channeling and electron diffraction experiments revealed that high fluence Fe implantation does not result in amorphisation but in recrystallisation of the matrix.

1. Introduction

This paper is part of a series of investigations concerning the microstructure and properties of solid solutions of $(1-0.x)(ZrO_2)$–$(0.x)(YO_{1.5})$, called afterwards ZYx, which are implanted with different metal ions [1–4]. In the present paper, the microstructure of Fe implanted ZYx is studied as a function of ion dose, Fe profile shape and thermal treatment. Special attention is paid to the chemical state of the implanted Fe, to precipitation phenomena and to the lattice damage recovery.

At elevated temperatures ZYx solid solutions are used as an oxygen ion conducting electrolyte in applications like oxygen sensors, oxygen pumps and fuel cells [5]. For these applications an electronically conducting electrode material on top of the ZYx specimen is necessary. Conventionally this material is Pt but mixed, i.e. electron and oxygen ion conducting materials are applied too [6–8]. By implantation of a suitable ion such a layer can also be obtained. The top layers formed by implantation have the advantage that they can be made very thin and that no sharp interface exists between the top layer and the ZYx specimen. Furthermore nonequilibrium compositions and microstructures can be realised. The electrochemical properties of the implanted materials are discussed elsewhere [1,10]. These and other properties of the implanted material depend on the microstructure, which is described in the present paper.

0168-583X/88/$03.50

2. Experimental

Polycrystalline ZY17 was prepared as described elsewhere [16]. Single crystals of ZY17 were obtained from Amplus-Crystal-Productions Verwaltung Gmbh 2 CO-K.G. Frankfurt a.M., FRG. ZYFe10 (ZY17 containing 10 mol% Fe_2O_3) was chemically prepared following the method as described in refs. [1] and [11]. Both single crystals and the ceramic yttria stabilised zirconia contain 1.5 wt.% Hf as a contamination. For RBS channeling experiments the monocrystalline material was oriented with the ⟨001⟩ direction at an angle of 6° with the normal of the surface of the disks.

Ion implantations were performed at room temperature with the isotope separator of the Laboratory for General Physics (LAN) of the State University of Groningen. Current densities < 2 μA cm^{-2} were applied with the ion beam normal to the specimen surface. The resulting depth profiles are given below.

TEM results were obtained with a Jeol-200 CX microscope on samples which were made thin enough by ion milling, starting from the unimplanted side, using a Cu grid as the support material.

The 5 MeV Van der Graaf generator in the LAN, producing a 2 MeV ^{4}He beam, has been used to perform the RBS experiments in combination with channeling.

For the Mössbauer experiments a drive with a source of ^{57}Co diffused in Rh (10 mC) was used in all experi-

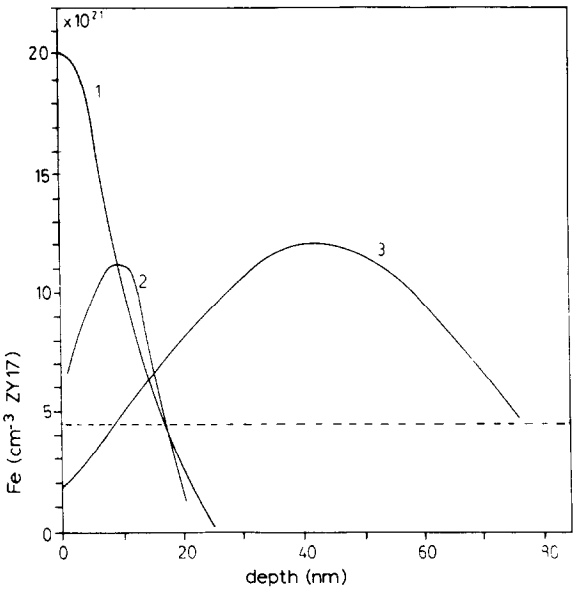

Fig. 1. Fe depth profiles in ZY16: (1) 8×10^{16} Fe cm^{-2}, 15 keV; (2) 2×10^{16} Fe cm^{-2}, 15 keV; (3) 8×10^{16} Fe cm^{-2}, 110 keV. The solubility level of Fe, calculated from the Mössbauer data in table 2, is indicated (- - -).

ments. This source served also as a reference in all Mössbauer experiments. For the CEMS (conversion electron Mössbauer spectroscopy) measurements, samples were implanted with ^{57}Fe ions and coated with a 20 nm thick C layer to avoid surface charging during the measurements. A negative velocity in the Mössbauer spectra means a movement of the source away from the sample counter.

The implanted samples were investigated with CEMS in the integral mode. A full account of the Mössbauer measurements and interpretation of the results is given in ref. [1] and will be published separately [13]. In this paper only a summary of the most important results is given.

Table 1
Sample codes used in the discussion of the results

Sample code	Implanted with		
	Dose [Fe cm^{-2}]	Voltage [kV]	
As-implanted:			*maximum concentration*
8–110	8×10^{16}	110	12×10^{21} Fe cm^{-3}
8– 15	8×10^{16}	15	20×10^{21} Fe cm^{-3}
2– 15	2×10^{16}	15	10×10^{21} Fe cm^{-3}
Annealed:			*subsequent treatment*
8–110– 400	8×10^{16}	100	400 °C, $\frac{1}{2}$ h
8– 15– 400	8×10^{16}	15	400 °C, $\frac{1}{2}$ h
2– 15– 400	2×10^{16}	15	400 °C, $\frac{1}{2}$ h
2– 15–1100	2×10^{16}	15	400 °C, $\frac{1}{2}$ h; 800 °C, 24 h; 1100 °C, $\frac{1}{2}$ h
ZYFe10	Chemically prepared ZY17 doped with 10 mol% Fe_2O_3 and quenched from 1500 °C		

3. Results and discussion

3.1. Compilation of microstructural investigations

Concentration profiles of Fe implanted in ZY16 are shown in fig. 1. The shape of these profiles does not change during thermal treatments up to 900 °C [3]. The different samples and their treatments are coded in table 1 and the main results of the microstructural investigations are compiled in table 2. Before discussing these combined results we start with a discussion of the results of each of the characterisation methods used.

Table 2
Compilation of the results obtained by TEM, RBS in combination with channeling and Mössbauer spectroscopy

Sample code	State of the implanted iron Fe atom [%]					Structure remarks
	Fe	Fe^0	Fe^{2+}	Fe_s^{3+}	Fe_h^{3+}	
As-implanted:						
8-110		55	29	16		amorphous (RBS)
8-15	27	14	25	34		microcryst. 30 nm
2-15			26	74		
Annealed:						
8-110-400				41	59	amorphous (RBS)
8-15-400				39	61	
2-15-400				56	44	
2-15-1100				57	43	
8-110-800						amorphous (RBS)
ZYFe10				100		

3.2. TEM results

Samples implanted with a high dose (table 1, code 8-15) show in the as-implanted state the formation of a granular substructure within the original grains (fig. 2) which is due to recrystallisation. The original grain boundaries become somewhat blurred and a substructure of small crystallites with a diameter of 30 nm is observable (note: original grain size $\geqq 0.5$ μm). This granular substructure is not present in the unimplanted part of the sample.

Diffraction patterns from these grains show, in addition to the reflections of cubic ZY, also the reflections of Fe_2O_3. All reflections appear as diffuse rings which indicates that both the ZY and the Fe_2O_3 are fine grained and randomly oriented. Dark field images of the Fe_2O_3 reflections show that very fine grained Fe_2O_3 precipitates (< 5 nm) are dispersed through the matrix. A microdiffraction pattern of these precipitates is depicted in fig. 3 and it shows the (012) reflections of hematite superimposed on the typical reflections of ZY.

The effect of thermal treatments on the size of the Fe_2O_3 precipitates has not as yet been investigated systematically. Preliminary results of treatments on 1100 °C ($\frac{1}{2}$ h) indicate a growth of the Fe_2O_3 microprecipitates from a diameter of 5 to 10 nm.

3.3. RBS in combination with channeling

The significant parameter in these experiments is χ_i, which is the ratio of the backscattering yields of the aligned beam and of the randomly incident beam for the ion species i (i = Zr, Fe or O). A value of $\chi_i = 1$ indicates complete randomisation of the sublattice of i, $\chi_i < 1$ indicates some ordering.

In the case of single crystalline ZY17 implanted with 8×10^{16} Fe cm^{-2}, 110 keV and annealed at 400 °C

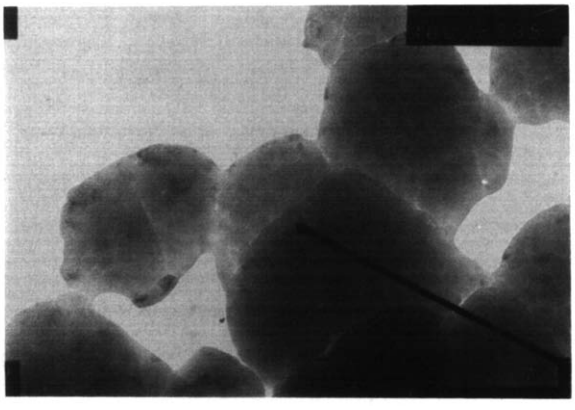

Fig. 2. TEM picture of ZY17 implanted with 8×10^{16} Fe cm^{-2}, 15 keV. The granular substructure within the original grains is clearly visible.

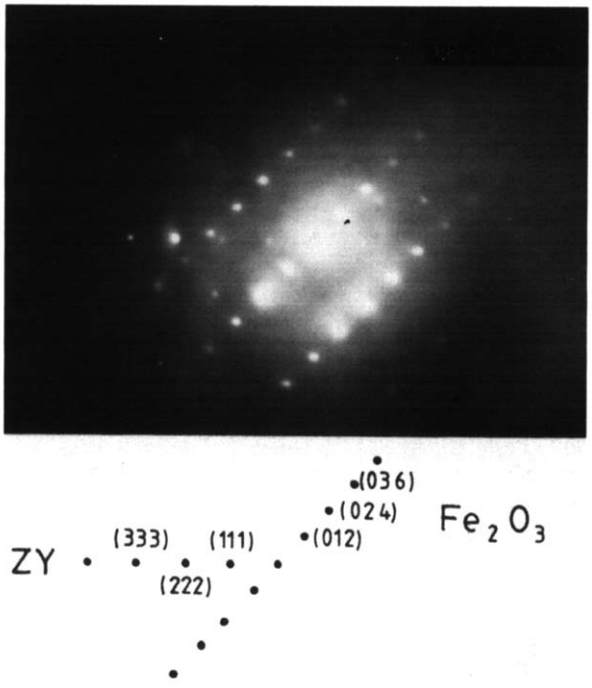

Fig. 3. Microdiffraction pattern obtained from the edge of an Fe implanted ZY crystal. It shows the superposition of diffraction spots of Fe_2O_3 and ZY.

(sample: 8-110-400, table 1), values of $\chi_{Zr} = 0.9$ were measured 15–23 nm below the surface and this is the area with maximum radiation damage (fig. 4). Ap-

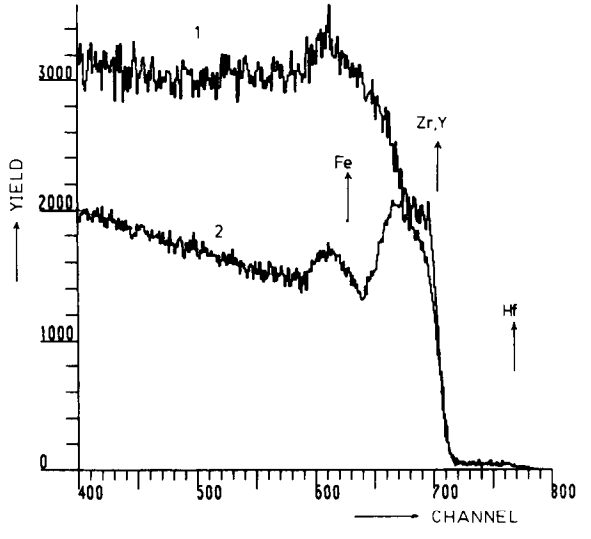

Fig. 4. Random (1) and ⟨110⟩ aligned (2) RBS spectrum of a Fe implanted (8×10^{16} Fe cm^{-2}, 110 keV) ZY17 single crystal after annealing at 400 °C for $\frac{1}{2}$ h (scattering angle: 150 °; 24 keV/ch.).

proximately the same value of χ_{Zr} is measured for the ZY17 single crystal after annealing at 800 °C.

Thus, according to RBS in combination with channeling, annealing in this temperature range apparently does not restore the ordering in the Zr sublattice. Together with the TEM results this can be explained in terms of recrystallisation of the single crystalline matrix in a random way.

This is in contrast to what has been measured for Yb implanted ZY17 single crystals [9]. The ⟨111⟩ crystal plane of an Yb implanted ZY17 single crystal shows an epitaxial growth of the implanted region after certain thermal treatments, and the Yb atoms are substitutionally incorporated in the Zr sublattice.

RBS experiments performed on polycrystalline ZY17 showed that the step height at the oxygen edge decreased after Fe implantation and again increased after oxidation at 400 °C of the implanted specimen. These changes indicate the loss of oxygen during implantation and the occurrence of a redox process during the low temperature anneal treatment.

3.4. Mössbauer spectroscopy

Transmission Mössbauer spectra were measured from chemically prepared ZYFe10 "standard" materials with known Fe concentration and (micro)structure [1]. The Mössbauer spectrum consists of a strong doublet with an isomer shift (IS) and a quadrupole splitting (QS) of respectively 0.23 mm s^{-1} and 1.24 mm s^{-1}. Although the resolution of the spectrum is low, the slightly higher absorption at velocities of −4.3 and 5.0 mm s^{-1} indicate that another component is present as well. These peaks are part of a sextuplet originating from Fe_2O_3 particles larger than 10 nm [14].

Conversion electron Mössbauer spectroscopy (CEMS) was applied to the ^{57}Fe implanted materials. First the CEMS spectra of the annealed samples will be discussed, since these samples have the closest resemblance to the chemically prepared ZYFe10 sample. A typical example of a CEMS spectrum of an annealed sample is shown in fig. 5. The computer fit of this spectrum yields an IS value comparable with that of ZYFe10, indicating that all of the iron is present in the Fe^{3+} state. The same conclusion holds for the samples implanted with larger doses and annealed at low temperature. Computer fits with only one Fe^{3+} site all yield curves with systematic deviations from the experimental curves. Therefore new fits were made assuming that two Fe^{3+} components were present with slightly different QS values. These two components are called afterwards Fe_s^{3+} and Fe_h^{3+}. Using two Fe^{3+} components, better fits were obtained. Moreover, all the spectra of annealed samples can now be described by a single set of parameters: the doublet Fe_h^{3+} with IS and QS values of 0.24–0.25 mm s^{-1} and 0.86–0.90 mm s^{-1} respectively

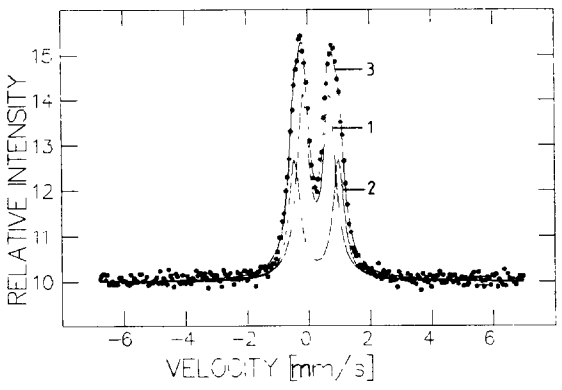

Fig. 5. CEMS spectrum of ZY17 implanted with 8×10^{16} Fe cm^{-2}, 15 keV annealed at 400 °C, ½ h (sample 8-15-400, table 1). The data are fitted with two components. (1) Fe_h^{3+}; (2) Fe_s^{3+}; (3) sum of (1) and (2).

and one doublet Fe_s^{3+} with IS and QS values of 0.24–0.25 mm s^{-1} and 1.43–1.48 mm s^{-1}. The Fe_s^{3+} doublet is ascribed to Fe^{3+} ions substitutionally incorporated for Zr^{4+} or Y^{3+} in the ZY lattice, and the Fe_h^{3+} doublet is ascribed to very small Fe_2O_3 precipitates (< 5 nm). The Fe_h^{3+} component is also found in MgO implanted with Fe [12] and it is explained by the occurrence of superparamagnetism in Fe_2O_3 particles smaller than 10 nm [14,15]. The characteristic sextuplet representing magnetical Fe_2O_3 reduces to a doublet with QS values of 0.78 mm s^{-1} when the Fe_2O_3 is very finely dispersed [14]. In MgO the observed QS value for these Fe_2O_3 particles was 0.89 mm s^{-1} [2], which is in good agreement with the QS values of Fe_h^{3+} observed in our work on ZY.

Finally a typical spectrum of an as-implanted specimen (8-15, table 1) is shown in fig. 6. In comparison to the Mössbauer spectrum depicted in fig. 5 two additional doublets and an additional sextuplet were observed. The doublet with IS and QS values of 0.91 and 2.01 mm s^{-1} respectively has been ascribed to Fe^{2+} and the doublet with IS = −0.07 and QS = 0.45 mm s^{-1} was ascribed to iron dimers [12]. The additional sextuplet was ascribed to relatively large iron particles.

Annealing of the as-implanted samples at relatively low temperatures (T = 300–400 °C) results in a rapid oxidation of iron to Fe^{3+}. This is in agreement with the observed increase in the oxygen content (RBS) and with the strong changes in electrical properties [10].

The relative abundance of each iron oxidation form has been calculated from the surface under the peaks in the spectra and is represented in table 2. Using this relative abundance together with the Fe depth profiles determined by RBS, a "solubility" level of implanted iron of $(4–5)\times10^{21}$ Fe cm^{-3} could be calculated (see fig. 1). This is about the same as found in the chemically prepared samples and is considerably larger than

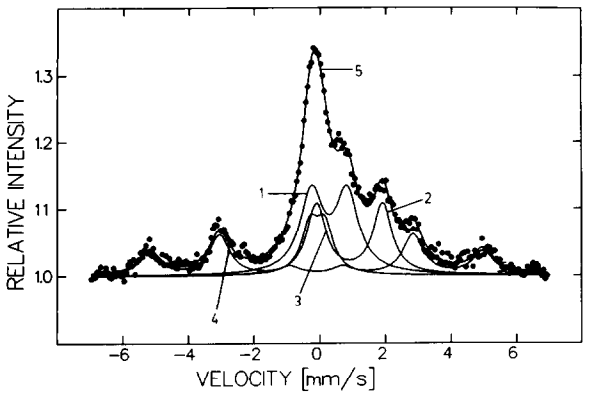

Fig. 6. CEMS spectrum of ZY17 as-implanted with 8×10^{16} Fe cm^{-2}, 15 keV (sample 8-15, table 1). The data are fitted with four components. (1) Fe^{3+} ($= Fe_h^{3+} + Fe_s^{3+}$); (2) Fe^{2+}; (3) Fe^0; (4) Fe (metallic particles); (5) Sum of (1), (2), (3) and (4).

the equilibrium solubility of Fe in ZY, which is about a factor of 3–4 lower [11].

4. Conclusions

From the investigations of the microstructure of Fe implanted ZY17 the following conclusions can be drawn:

(1) ZY17 material maintains its crystalline structure after high dose Fe implantation. However, recrystallisation of the ZY lattice occurs which results, in the case of ZY17 ceramics, in an intragranular substructure (TEM) and, in the case of ZY17 single crystals, in a polycrystalline surface layer (RBS).

(2) In the as-implanted state, Fe^+ implanted ZY17 contains metallic iron particles, Fe^0 dimers, and Fe^{2+} and Fe^{3+} ions. Their relative abundance depends on the implantation conditions (CEMS).

(3) During the thermal treatment of the as-implanted material at 400 °C, a rapid oxidation occurs. All different oxidation states of the iron present in the as-implanted state are converted to Fe^{3+} (CEMS).

(4) The maximum concentration of Fe^{3+} that can be substitutionally incorporated on Zr^{4+} lattice sites in the implanted ZY17 matrix after thermal treatment (400 °C, $\frac{1}{2}$ h) is about $(4–5)\times10^{21}$ Fe cm^{-3}. This is the same level as has been observed for substitutionally dissolved Fe^{3+}, metastably present in chemically prepared ZY17.

(5) In Fe implanted samples with iron concentrations exceeding this level, exsolution of Fe_2O_3 is observed after thermal treatments at 400 °C for $\frac{1}{2}$ h. The diameter of these hematite particles is less than 5 nm. They are completely dispersed in the ZY17 crystals (CEMS, TEM).

The authors are grateful to Dr. E.H. du Marchie van Voorthuysen and J.J. Smit of the State University of Groningen for the ion implanter facilities. We also want to thank Prof. Dr. L. Niesen for his help with the Mössbauer experiments and Dr. Ir. J. Beyer for his assistance with the TEM measurements.

The investigations were supported by the Netherlands Foundations for Chemical Research (SON) with financial aid from ZWO. We acknowledge the financial support from the CNRS.

References

[1] D. Scholten, PHD Thesis, University of Twente, Enschede The Netherlands (1987).
[2] D. Scholten and A.J. Burggraaf, Radiat. Eff. 97 (1986) 191.
[3] D. Scholten and A.J. Burggraaf, Surf. Interface Anal. 9 (1986) 467.
[4] D. Scholten and A.J. Burggraaf, Sol. Stat. Ionics 16 (1985) 147.
[5] E.C. Subbarao and H.S. Maiti, Sol. Stat. Ionics 11 (1984) 317.
[6] M.P. van Dijk, PhD Thesis, University of Twente, Enschede, The Netherlands (1985).
[7] M.P. van Dijk, K.J. de Vries and A.J. Burggraaf, Sol. Stat. Ionics 21 (1986) 173.
[8] Y. Takasu, T. Sugini and Y. Matsuda, J. Appl. Electrochem. 14 (1984) 79.
[9] C. Cohen, J. Siejka, M. Berti, A.V. Drigo, M. Croset and M.M. Tosic, Radiat. Eff. 64 (1982) 221.
[10] A.J. Burggraaf, D. Scholten and K.J. de Vries, Proc. 6th Int. Meeting on Solid State Ionics, Garmisch Partenkirchen (1987) to be published in a special issue of Sol. Stat. Ionics.
[11] A.J. Burggraaf, A.J.A. Winnubst and D. Scholten, to be publishcd.
[12] A. Perez, J.P. Dupin, O. Massenet, G. Marest and P. Bussière, Radiat. Eff. 52 (1980) 127.
[13] A.J. Burggraaf, D. Scholten and L. Niessen, to be published.
[14] W. Kundig, H. Bömmel, G. Constabaris and G.H. Lindquist, Phys. Rev. 142 (1966) 327.
[15] J.M. Friedt and J.P. Adloff, Compt. Rend. 226C (1986) 1733.
[16] M.A.C.G. van de Graaf and A.J. Burggraaf, Advances in Ceramic, vol. 12, eds. N. Claussen, M. Rühle and A.H. Heuer (The American Ceramic Society, Columbus, 1984) p. 744.